

# Study of growth and oxidation of vanadium films on $\alpha$ -Fe<sub>2</sub>O<sub>3</sub>(0001)

Chang-Yong Kim \*, Michael J. Bedzyk

*Department of Materials Science and Engineering, Northwestern University, Evanston, IL 60208, USA*  
*Institute for Environmental Catalysis, Northwestern University, Evanston, IL 60208, USA*

Received 3 October 2005; received in revised form 23 March 2006; accepted 14 April 2006  
Available online 2 June 2006

## Abstract

Electronic structures of the vanadium/vanadium-oxide films supported on  $\alpha$ -Fe<sub>2</sub>O<sub>3</sub>(0001) were studied by using X-ray photoemission spectroscopy. The vanadium films were grown by evaporation of metallic vanadium at room temperature. The as-deposited V had a 3+ oxidation state and the  $\alpha$ -Fe<sub>2</sub>O<sub>3</sub>(0001) surface was reduced at the initial coverage. After complete reduction of interface iron atoms, metallic V started to grow at a vanadium coverage greater than 2/3 monolayer. The V<sub>2</sub>O<sub>5</sub> film was prepared by exposing the pre-deposited vanadium film to the atomic oxygen at room temperature. Converting to the V<sub>2</sub>O<sub>5</sub> film was accompanied by re-oxidation of the  $\alpha$ -Fe<sub>2</sub>O<sub>3</sub> at the interface. The reduction and re-oxidation of interfacial iron manifest electron transfer between the adsorbed vanadium and substrate.  
© 2006 Elsevier B.V. All rights reserved.

*Keywords:* Vanadium oxide; X-ray photoelectron spectroscopy (XPS); Oxidation; Iron oxide

## 1. Introduction

Material systems of metals or metal-oxides supported on different type of oxides have been studied extensively due to their wide applications in heterogeneous catalysis and gas sensors [1]. Despite this considerable interest, the morphology of the supported metal or metal oxide, the active sites and role of supporting oxides in catalytic reaction need to be explored further to design and to understand a new types of catalysis for specific reactions.

Supported vanadium oxide has been used in the manufacture of important chemicals and in the reduction of environmental pollution [2]. In supported vanadium oxide catalysis, a phenomenon known as monolayer catalysis has been reported [3]. Here a submonolayer vanadium oxide film supported by appropriate oxide displays greater catalytic activity when compared to multilayer vanadium oxide films. The monolayer catalysis indicates significant role of the supporting oxide substrate. Significance of reducibility of the supporting oxide has also been proposed [4]. In many cases, the catalytic activity of vanadium oxide has an oxidation state dependency and the

existence of 5+ oxidation state is crucial for catalytic reactions [5,6].

There have been significant efforts to prepare vanadium penta-oxide on various metal-oxide substrates due to this significance of 5+ vanadium catalysts [7]. So far, the effort to grow a V<sub>2</sub>O<sub>5</sub> film on a different oxide substrate was only successful for growing monolayer films on TiO<sub>2</sub>(110) [6, 8] and CeO<sub>2</sub>(111) [9] substrates. The previous efforts can be categorized either as post-annealing of a pre-deposited vanadium film in relatively high oxygen partial pressure of 10<sup>-3</sup> Torr [6, 9] or as co-dosing of VOCl<sub>3</sub> and water followed by annealing in 2 × 10<sup>-6</sup> Torr of molecular oxygen [8]. The V<sub>2</sub>O<sub>3</sub> films appeared to be the most stable vanadium oxide form grown on many oxides substrate [7,9–12].

As most stable form of iron oxide,  $\alpha$ -Fe<sub>2</sub>O<sub>3</sub> (hematite) has wide application in fields of heterogeneous catalysis, corrosion and gas sensing [1]. Vanadium oxide on  $\alpha$ -Fe<sub>2</sub>O<sub>3</sub> is an interesting system since V<sub>2</sub>O<sub>3</sub> and  $\alpha$ -Fe<sub>2</sub>O<sub>3</sub> are isostructural, as both share the corundum structure. An oxidation of interface atoms has been observed in vanadium films grown on oxide substrates [11–14]. In films grown on corundum substrates, Al<sub>2</sub>O<sub>3</sub> [11] and Cr<sub>2</sub>O<sub>3</sub> [14], vanadium atoms in metallic and 3+ oxidation state have been observed. Evolution of oxidation state of vanadium as function of film thickness could provide insight of interface oxidation in metal/oxide system.

\* Corresponding author. Department of Materials Science and Engineering, Northwestern University, Evanston, IL 60208, USA.

E-mail address: [cykim@northwestern.edu](mailto:cykim@northwestern.edu) (C.-Y. Kim).

By exposing pre-deposited vanadium films to an atomic oxygen gas flow, we were able to prepare multi- and sub-monolayer vanadium penta-oxide supported on a  $\alpha\text{-Fe}_2\text{O}_3(0001)$  substrate. In this paper, we report about the electronic structures of the vanadium and vanadium oxide films grown on a  $\alpha\text{-Fe}_2\text{O}_3(0001)$  substrate.

## 2. Experimental details

The vanadium deposition and X-ray photoelectron spectroscopy (XPS) measurements were carried out in an ultra-high vacuum (UHV) chamber by using a Knudsen-cell evaporator, a dual anode X-ray source and a PHI hemispherical electron energy analyzer. The chamber was also equipped with low energy electron diffraction (LEED) and gas sources. The base pressure of the chamber was  $5 \times 10^{-11}$  Torr.

The  $\alpha\text{-Fe}_2\text{O}_3(0001)$  sample was purchased from Commercial Crystal Laboratories as a 1.0-mm-thick polished wafer. Degreased samples were mounted on a molybdenum sample holder, which could be heated from the backside by thermal radiation from a hot tungsten filament. The sample temperature was monitored using optical pyrometer and a thermocouple attached near the sample holder. The clean surface was prepared by annealing the sample at 450 °C under a stream of atomic oxygen gas. The chamber pressure of  $1 \times 10^{-6}$  Torr was kept during sample annealing and also during cooling down to room temperature. The atomic oxygen flow was produced by passing molecular oxygen gas through a refractory capillary tube (MANTIS Deposition, TC50, 60 W power) heated to  $975 \pm 50$  °C by an e-beam bombardment method. Due to the directional flow of the gas actual oxygen partial pressure at the sample surface would be higher than the chamber pressure. The ratio of atomic oxygen to molecular oxygen determined by quadrupole mass spectrometer was 1.5. After annealing in the atomic oxygen environment for 30 min a sharp  $(1 \times 1)$  LEED pattern was observed from the surface. No carbon contamination was detected in XPS. The main impurities of Ca and K from the natural crystal were detected in XPS with less than 0.05 monolayer (ML).

The vanadium (99.9 %, Goodfellow) was successively deposited on to the  $\alpha\text{-Fe}_2\text{O}_3(0001)$  substrate by means of a Knudsen cell evaporator. During the deposition sample was at room temperature and chamber pressure was better than  $2 \times 10^{-9}$  Torr. After characterizing as-deposited vanadium films with XPS, vanadium oxides were then prepared by exposing the deposited vanadium to the atomic oxygen. During the atomic oxygen exposure sample was kept at room temperature to avoid a possible inter-diffusion of vanadium to the  $\alpha\text{-Fe}_2\text{O}_3$  substrate.

XPS measurements were performed with a non-monochromatic Al K $\alpha$  X-ray source and with a hemispherical electron energy analyzer. No charging from the sample was observed during the measurements. The work function changes were measured from shifts of the secondary electron cut-offs of the XP spectra taken from the negatively biased sample.

## 3. Results and discussion

Fig. 1 shows how the work function changes with increasing film thickness. The work function of the clean  $\alpha\text{-Fe}_2\text{O}_3(0001)$  surface was measured from the difference between the excitation energy (1486.6 eV for Al K $\alpha_{1,2}$ ) and the entire width of the XP spectra ( $KE(E_F) - KE(E_{\text{cut-off}})$ ) obtained from negatively biased sample. The measured work function of 5.38 eV is similar to previously reported theoretical and experimental values [15,16]. From different types of iron oxides similar work functions were observed, FeO(111) 5.90 eV and Fe<sub>3</sub>O<sub>4</sub>(111) 5.52 eV [17]. As the V deposition proceeds the work function change shows three distinct stages. In an early stage of deposition, the substrate work function decreases rapidly. Then the work function increases slowly after reaching a minimum and approaches 3.95 eV. Finally, the work function of the thick film decreases again and approaches 3.81 eV. It is worthwhile to note that reported work function of bulk vanadium metal varies between 4.10 eV and 4.65 eV [13,18,19].

The initial work function reduction can be understood as a result of electron donation from deposited vanadium to  $\alpha\text{-Fe}_2\text{O}_3$  surface layers. This interpretation is supported by changes in the oxidation state of V and interface Fe as described below. In analogy to an alkali metal system [20] the observed work function minimum can be explained by de-polarization of a vanadium-induced dipole moments due to an increasing interaction between the dipoles at a higher coverage. In alkali metal system the work function increases as result of back-donation of electrons to the deposited alkali metal. Adsorption site change and morphology change (including island formation which occurs as the coverage increases) can also affect surface work function [21]. As the vanadium coverage increases, LEED patterns changed to a dimmed  $(1 \times 1)$  with increased background intensities. The dimmed  $(1 \times 1)$  pattern was maintained even after the  $\alpha\text{-Fe}_2\text{O}_3$  substrate is covered by a thick vanadium film, which implies a three-dimensional vanadium island growth. Since the spill-over of electron at step edge creates dipole

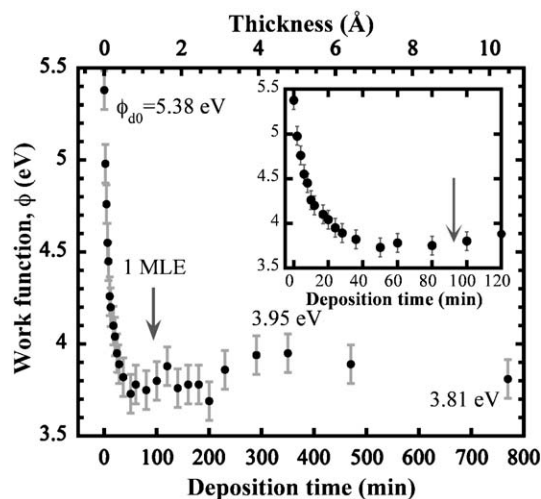


Fig. 1. The work function as a function of deposition time and estimated V thickness. The inset shows the rapid decrease of the work function at the early stage of deposition. The arrows mark 1.0 monolayer equivalent V coverage.

moments opposite to the flat surface, steps cause overall reduction of work function [22]. Deviation of work function from bulk value for the thick film can be attributed to the 3D vanadium island formation which introduces step edges.

Along with the work function changes, there were corresponding changes in Fe 2p and V 2p XP spectra. As manifested in the Fe 2p spectra shown in Fig. 2, donated electrons from the deposited vanadium were transferred to the Fe. This subsequently changes the oxidation state of the Fe from +3 to +2. In addition to a small shift (1 eV at most) in the peak position, the 2p XP spectra from Fe ions have a distinct oxidation-state-dependent satellite features that indicated as arrows in Fig. 2. The 2p spectrum from the Fe<sup>2+</sup> ions have satellite peaks separated toward higher binding energy by 6 eV from the main peaks and the Fe<sup>3+</sup> ions have satellites at 8 eV higher binding energy sides of the main peaks [23–25]. As the vanadium coverage increases, the contribution from the Fe<sup>2+</sup> ions increases and the 2p spectrum changes gradually from that of Fe<sup>3+</sup> to Fe<sup>2+</sup> ion.

The vanadium deposits are oxidized after donating electrons to the  $\alpha$ -Fe<sub>2</sub>O<sub>3</sub> substrate. The binding energy of 515.7 eV of the V 2p<sub>3/2</sub> peak in a low coverage region is close to the vanadium in the 3+ oxidation state (V<sup>3+</sup> at 515.85 eV, V<sup>5+</sup> at 517.2 eV [26] and V<sup>0</sup> at 512.2 eV [27]). The binding energy of the V<sup>3+</sup> peak does not change in a thicker film (dotted guideline in Fig. 3). At a higher coverage additional peak is developed showing characteristics of a spectrum from a metal that has a continuous electron energy loss tail in its higher binding energy side. As the vanadium coverage increases, the binding energy of the metallic peak changes slowly (solid guideline in Fig. 3) from 513.3 eV to 512.8 eV. The continuous shift of binding energy indicates that the metallic peak might be originated from vanadium clusters of which the size increases as coverage increases [28].

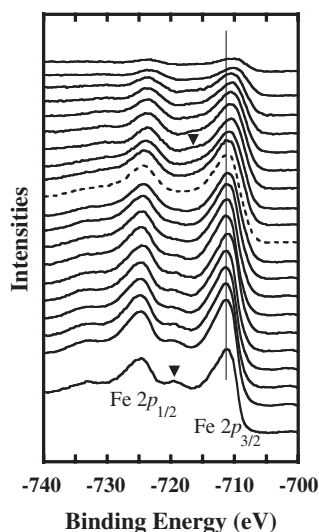


Fig. 2. Change of Fe 2p spectra with increasing vanadium coverage with the clean  $\alpha$ -Fe<sub>2</sub>O<sub>3</sub> surface spectrum at the bottom. Dashed line corresponds to spectrum from c.a. 1 MLE vanadium film. Arrows indicate characteristic satellite peaks from 3+ and 2+ iron ions. Vertical line is to guide the eyes for small peak position shifts.

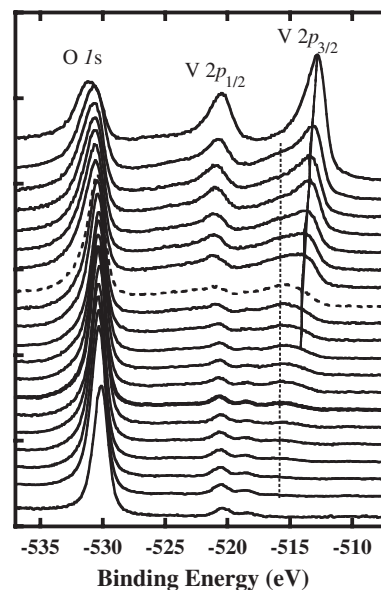


Fig. 3. O 1s, V 2p spectra with increasing vanadium coverage. Guidelines are drawn to connect the oxide peaks with constant binding energy and the metallic peaks with shifting binding energy.

The XP spectra in the valence band region are shown in Fig. 4. Along with the development of V<sub>2</sub>O<sub>3</sub> that shows metallic behavior, the intensities at the Fermi level increase. As the metallic V peak starts to grow, the intensity at the Fermi level increases further. Especially the spectrum from the second thickest film shows the characteristics of a metal spectrum, which has featureless plateau from 4 eV up to the Fermi level.

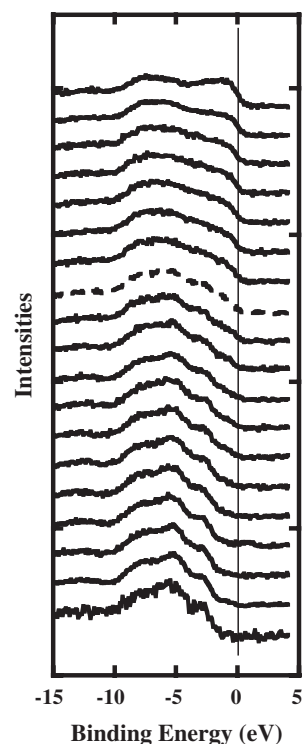


Fig. 4. Valence band spectra with increasing V coverage.

For quantitative analysis, the Fe 2p spectra were reconstructed from reference spectra from Fe<sup>3+</sup> and Fe<sup>2+</sup> ions. The Fe 2p spectrum from clean  $\alpha$ -Fe<sub>2</sub>O<sub>3</sub>(0001) surface was used for Fe<sup>3+</sup> reference. The Fe<sup>2+</sup> reference spectrum was taken from Ar ion sputtered  $\alpha$ -Fe<sub>2</sub>O<sub>3</sub>(0001) surface where majority of subsurface Fe ions are in 2+ oxidation state [23,29]. The sputtering was performed with 500 eV ion energy at a 1.5  $\mu$ A sample current for 20 min. The iron metal peak was not observed from the sputtered surface. The background due to inelastic scattering of photoelectrons was calculated with the Tougaard formalism [30] and subtracted from the measured spectra. The differential inelastic cross section  $K(E,T)$  for the photoelectron with primary energy  $E$  and energy loss  $T$  was approximated to a universal cross section as  $\lambda K(T) = BT/(1 + (CT)^2)$ , where  $\lambda$  denotes the inelastic electron attenuation. The constant value for  $C$  was taken as 1643 eV<sup>2</sup> from the literature [30]. The value of  $B$  was selected so that the universal formula can give reasonable background for a spectrum of a wide binding energy region from the clean surface. The selected constant  $B$  of 2380 eV<sup>2</sup> is comparable to values used by other groups for iron oxide studies [31,32]. As an example of the reconstruction, the Fe 2p spectra for 50 min of vanadium deposition are shown in Fig. 5. The measured spectrum was reconstructed with contributions of 43% of Fe<sup>3+</sup> and 57% Fe<sup>2+</sup> reference spectra. Fig. 6a shows integrated intensities of measured Fe 2p spectra with background correction and the ratio of the Fe<sup>3+</sup> to the Fe<sup>2+</sup> reference spectra used to compose the spectra. The integrated intensities of Fe 2p photoelectron diminished with increasing deposition time. The vanadium film thickness was estimated through fitting of an attenuation of the substrate Fe 2p photoelectron signal to  $\exp(-t/\lambda_{Fe})$  and the growth of metal V 2p<sub>3/2</sub> intensities to  $1 - \exp(-(t - t_0)/\lambda_V)$ . The  $\lambda$ ,  $t$  and  $t_0$  denote effective attenuation length, total film thickness and the onset thickness at which the metal V appears, respectively. The best fit gives deposition rate of 0.014 Å/min with effective attenuation lengths of 14.3 Å and 17.0 Å for Fe

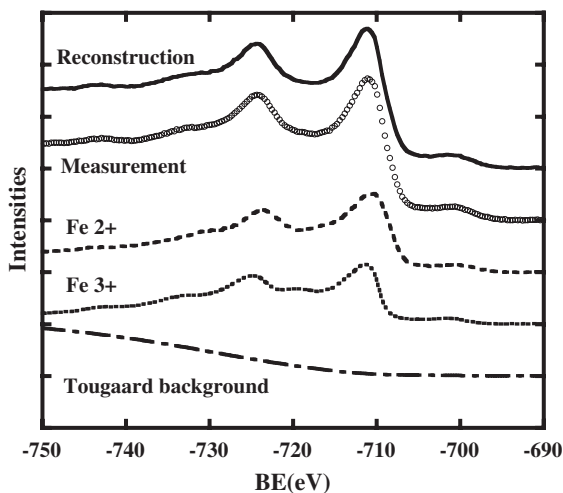


Fig. 5. Fe 2p spectra of V/ $\alpha$ -Fe<sub>2</sub>O<sub>3</sub>(0001), V deposited at room temperature for 50 min. Circle: raw XPS data. Dashed line: contribution for Fe<sup>2+</sup> ions. Dotted line: contribution from Fe<sup>3+</sup> ions. Dash-dotted line: Tougaard background. For the reconstruction 43% Fe<sup>3+</sup> and 56% Fe<sup>2+</sup> contributions were used.

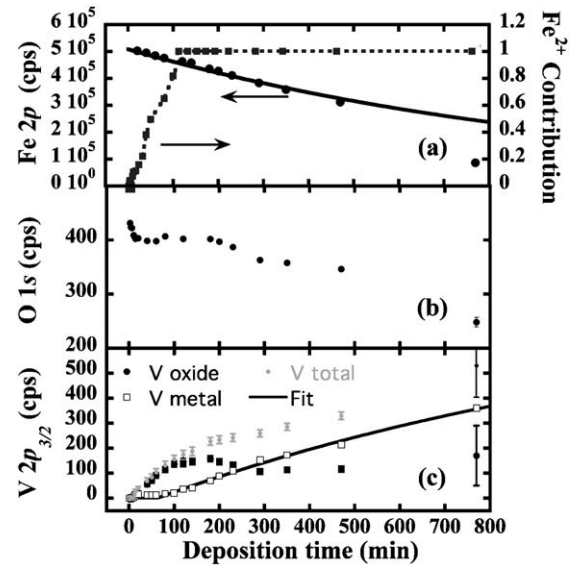


Fig. 6. (a) Integrated intensities of Fe 2p spectra (filled circle) and Fe<sup>2+</sup> contribution to Fe 2p spectra (filled square) as function of deposition time. Integrated intensities of O 1s (b) and V 2p<sub>3/2</sub> (c). Solid lines represent fitting result for changes of Fe 2p and metal V 2p intensities caused by the vanadium film growth.

2p and V 2p<sub>3/2</sub> photoelectrons, respectively [33]. This estimation should be taken as an approximation since it is accurate only for layer by layer film growth. The film thickness was converted to coverage based on V density 6.11 g/cm<sup>3</sup>. The coverages are referred in “monolayers equivalent” (MLE) to account V island formation. 1 MLE of vanadium was defined to be  $0.91 \times 10^{15}$  atoms/cm<sup>2</sup> which is the density of Fe atoms in the  $\alpha$ -Fe<sub>2</sub>O<sub>3</sub>(0001) surface.

The oxygen and vanadium spectra were fitted with a Doniac-Sunjic lineshape for metallic vanadium peaks and with a Voigt function (Gaussian convoluted Lorentzian) for the other oxide peaks. In both cases a Shiely-type background was used. Unfortunately, the V 2p XP spectra excited by Al K $\alpha_{1,2}$  overlap with O 1s peaks excited by Al K $\alpha_3$  and K $\alpha_4$ . The relative positions and intensities of the O 1s peaks excited by K $\alpha_{3,4}$  and K $\alpha_{1,2}$  were obtained by fitting the spectra from the clean surface. The obtained fixed relation of position and intensity was used during fitting procedure to take account excitations by K $\alpha_{3,4}$ . As shown in Fig. 6(c), the V 2p metallic peak intensities started to develop above a thickness of 2/3 MLE where the substrate Fe 2p are mostly in 2+ states. Following an initial growth, the vanadium oxide peak intensities approach constant values after showing a maximum at about 150-min deposition. The behavior of the vanadium oxide photoelectron intensities could be due to an oxidation of the outer metallic vanadium surface layers by residual oxygen in the UHV chamber. The existence of the surface vanadium oxide layer can be seen from the non-vanishing oxygen signal (Fig. 6(b)) even after the Fe signal attenuated to background level. Contrary to the Fe photoelectrons, the intensities of the O 1s peaks were not attenuated to zero but approach a finite value.

The vanadium deposition on  $\alpha$ -Fe<sub>2</sub>O<sub>3</sub>(0001) can be summarized as follows. At the early stage of film growth,

the deposited vanadium is oxidized to  $V^{3+}$  after donating electrons to the substrate. The electron transfer also causes the work function to decrease, and reduction of the substrate Fe ion from a 3+ to 2+ oxidation state. Above a film thickness of 2/3 MLE, the near surface Fe ions are mostly in a 2+ oxidation state and the vanadium metal clusters start to grow.

As shown in Fig. 7(a), exposure to a flow of atomic oxygen at room temperature oxidized a thick vanadium film resulted from 770 min of accumulated V deposition. The V 2p<sub>3/2</sub> XP spectrum showed a single peak at the binding energy of 517.0 eV which can be assigned to V<sub>2</sub>O<sub>5</sub>. The assignment of the

oxidized film to V<sub>2</sub>O<sub>5</sub> is evident from a sharp feature of the V 2p spectrum that originates from a d<sup>0</sup> electronic configuration of the 5+ vanadium ions. To check the change of the V<sup>3+</sup> component in the sub-monolayer film, the 0.64 MLE vanadium film was prepared and exposed to the atomic oxygen flow at room temperature. The vanadium deposits in the 3+ oxidation state also fully oxidize to the 5+ oxidation state upon atomic oxygen exposure (Fig 7(b)).

Interestingly, the Fe 2p spectrum composed from a mixture of 3+ and 2+ iron ions with the as-deposited 0.64 MLE film changed to a spectrum from pure 3+ iron ions after the atomic oxygen exposure (Fig. 7(c)). Similar reduction and re-oxidation of substrates has been reported in systems of vanadium films on other types of metal oxides [9,13,14]. For the 0.64 MLE film, the exposure to the atomic oxygen source introduced distinct energy gap in valence band region.

The thermal stability of vanadium oxide films is usually hampered by the inter-diffusion of the vanadium deposits into the  $\alpha$ -Fe<sub>2</sub>O<sub>3</sub> substrate upon heating of the substrate. Since the inter-diffusion behavior of metals and their oxide form can differ, we annealed vanadium oxide films prepared by the atomic oxygen exposure. Interestingly, the multilayer V<sub>2</sub>O<sub>5</sub> film is stable upon annealing in the sense that the V<sup>5+</sup> does not convert to V<sup>3+</sup> contrary to the V<sub>2</sub>O<sub>3</sub> multilayer formation on CeO<sub>2</sub>(111) substrate. Post-annealing under  $1 \times 10^{-3}$  Torr O<sub>2</sub> converted multilayer vanadium films on a CeO<sub>2</sub>(111) to V<sub>2</sub>O<sub>3</sub> films [9]. Although there was a decrease of the V 2p XPS intensities caused either by diffuse-in or desorption of vanadium, the vanadium penta-oxide prepared on  $\alpha$ -Fe<sub>2</sub>O<sub>3</sub> (0001) with atomic oxygen exposure was stable up to 450 °C (Fig. 7(a)).

#### 4. Summary

The electronic structure of vanadium and vanadium oxide films prepared on a hematite ( $\alpha$ -Fe<sub>2</sub>O<sub>3</sub>)(0001) substrate has been studied. At submonolayer coverage, the vanadium deposits achieve a 3+ oxidation state by donating electrons to the substrate. The transferred electrons caused a substrate work function decreases and a reduction of the substrate Fe ions from 3+ to 2+ oxidation states. Metallic vanadium started to grow after whole reducible interface Fe ions are changed to 2+. Exposure of the vanadium films to atomic oxygen converted the films to vanadium penta-oxide films. Re-oxidation of substrate Fe ions was observed during the formation of sub-monolayer vanadium penta-oxide. The observed reduction and re-oxidation of the supporting  $\alpha$ -Fe<sub>2</sub>O<sub>3</sub> imply a significant role of a supporting oxide in heterogeneous catalysis where reduction and re-oxidation of vanadium oxide catalysts would take place during catalytic reaction.

#### Acknowledgement

This research is supported by the Chemical Sciences, Geosciences and Biosciences Division, Office of Basic Energy Sciences, Office of Science, U.S. Department of Energy, Grant No. DE-FG02-03ER15457. The work made

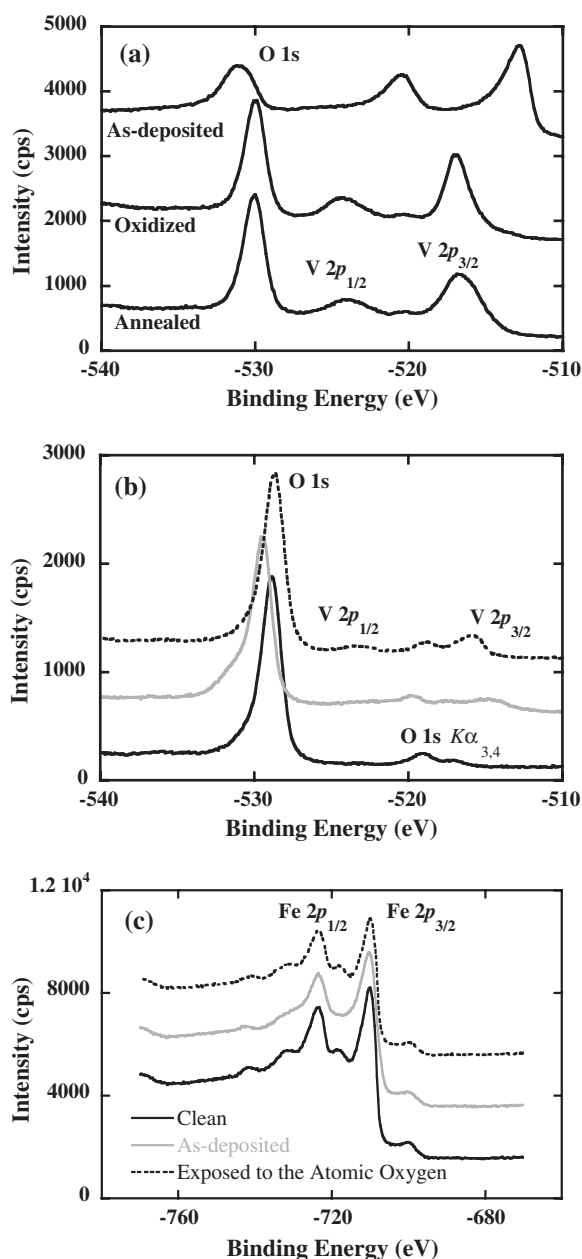


Fig. 7. (a) Effects of the atomic oxygen exposure and vacuum annealing in O 1s and V 2p spectra of vanadium film produced by 770 min of deposition. Changes in O 1s and V 2p spectra (b) and Fe 2p spectra (c) caused by the atomic oxygen exposure to submonolayer vanadium film.

use of Northwestern University Central Facilities supported by the MRSEC program of the NSF (DMR-0520513).

## References

- [1] V.E. Henrich, P.A. Cox, *The Surface Science of Metal Oxides*, University Press, Cambridge, 1994.
- [2] B.M. Weckhuysen, D.E. Keller, *Catal. Today* 78 (2003) 25.
- [3] G.C. Bond, S.F. Tahir, *Appl. Catal.* 71 (1991) 1.
- [4] N. Magg, J.B. Giorgi, T. Schroeder, M. Baumer, H.J. Freund, *J. Phys. Chem. B* 106 (2002) 8756.
- [5] Q.G. Wang, R.J. Madix, *Surf. Sci.* 496 (2002) 51.
- [6] G.S. Wong, M.R. Concepcion, J.M. Vohs, *Surf. Sci.* 526 (2003) 211.
- [7] S. Surnev, M.G. Ramsey, F.P. Netzer, *Prog. Surf. Sci.* 73 (2003) 117.
- [8] Q.G. Wang, R.J. Madix, *Surf. Sci.* 474 (2001) L213.
- [9] G.S. Wong, J.M. Vohs, *Surf. Sci.* 498 (2002) 266.
- [10] J. Biener, M. Baumer, R.J. Madix, *Surf. Sci.* 432 (1999) 178.
- [11] J. Biener, M. Baumer, R.J. Madix, P. Liu, E.J. Nelson, T. Kendelewicz, G.E. Brown, *Surf. Sci.* 441 (1999) 1.
- [12] A. Atrei, T. Cecconi, B. Cortigiani, U. Bardi, M. Torrini, G. Rovida, *Surf. Sci.* 513 (2002) 149.
- [13] Z.M. Zhang, V.E. Henrich, *Surf. Sci.* 277 (1992) 263.
- [14] W.D. Xiao, K. Xie, Q.L. Guo, E.G. Wang, *J. Phys.: Condens. Matter* 14 (2002) 6321.
- [15] E.R. Batista, R.A. Friesner, *J. Phys. Chem. B* 106 (2002) 8136.
- [16] C. Gleitzer, J. Nowotny, M. Rekas, *Appl. Phys. A* 53 (1991) 310.
- [17] W. Ranke, W. Weiss, *Surf. Sci.* 414 (1998) 236.
- [18] T. Valla, P. Pervan, M. Milun, K. Wandelt, *Surf. Sci.* 374 (1997) 51.
- [19] M. Kralj, P. Pervan, M. Milun, *Surf. Sci.* 423 (1999) 24.
- [20] H.P. Bonzel, A.M. Bradshaw, G. Ertl (Eds.), *Physics and Chemistry of Alkali Metal Adsorption*, Elsevier, Amsterdam, 1989.
- [21] J. Neugebauer, M. Scheffler, *Phys. Rev. Lett.* 71 (1993) 577.
- [22] R. Smoluchowski, *Phys. Rev.* 60 (1941) 661.
- [23] C.R. Brundle, T.J. Chuang, K. Wandelt, *Surf. Sci.* 68 (1977) 459.
- [24] N. Beatham, A.F. Orchard, G. Thornton, *J. Phys. Chem. Solids* 42 (1981) 1051.
- [25] A. Fujimori, M. Saeki, N. Kimizuka, M. Taniguchi, S. Suga, *Phys. Rev. B* 34 (1986) 7318.
- [26] M. Demeter, M. Neumann, W. Reichelt, *Surf. Sci.* 454 (2000) 41.
- [27] A. Maetaki, K. Kishi, *Surf. Sci.* 411 (1998) 35.
- [28] G.K. Wertheim, *Z. Phys. B* 66/1 (1987) 53.
- [29] T.J. Chuang, C.R. Brundle, K. Wandelt, *Thin Solid Films* 53 (1978) 19.
- [30] S. Tougaard, *Solid State Commun.* 61 (1987) 547.
- [31] P.C.J. Graat, M.A.J. Somers, *Appl. Surf. Sci.* 101 (1996) 36.
- [32] S.J. Roosendaal, PhD thesis, University of Utrecht, 1999.
- [33] C.J. Powell, A.A. Jablonski, *NIST Electron Effective-Attenuation Length Database-Version 1.0*, National Institute of Standards and Technology, Gaithersburg, MD, 2001.